NASA Technical Memorandum 103121

Acquisition and Correlation of Cryogenic Nitrogen Mass Flow Data Through a Multiple Orifice Joule-Thomson Device

S. Stephen Papell
Analex Corporation
NASA Lewis Research Center
Fairview Park, Ohio

and

Naseem H. Saiyed and Ted W. Nyland
National Aeronautics and Space Administration
Lewis Research Center
Cleveland, Ohio

May 1990

(NASA-TM-103121) ACQUISITION AND CORRELATION OF CRYOGENIC NITROGEN MASS FLOW DATA THROUGH A MULTIPLE ORIFICE JOULE-THOMSON DEVICE (NASA) 23 p CSCL 20D N90-27711
Unclas
G3/34 0291590

NASA

long as the J-T coefficient for the process is positive. The use of a Visco Jet to achieve this (J-T) effect for aerospace systems has been proposed (ref. 1) because of its simplicity. Its primary advantage over a valve is the absence of moving parts. Its major disadvantage is the decreased flexibility in the operating flow rates. Visco Jets (ref. 2) were designed as miniature hydraulic flow components using a "multiple orifice" concept to induce a pressure drop in a line. The flow path includes many orifices in series containing spin chambers that induce significant pressure drops. This design allows the use of holes five times larger than a single hole required to produce the same pressure drop. The larger hole reduces the possibility of clogging due to solid contaminants in the line. The onset of cavitation is also minimized by the reduced velocity in the jet due to the larger size hole. The resistance to flow is measured in liquid ohms - or Lohms, a term created and used by the manufacturer. This term is included in an equation from reference 2 that predicts single-phase liquid flow rates for many fluids. The form of the equation, defined as the Lee equation, follows:

$$\dot{m} = \left(\frac{10\ 000}{\text{Lohm}}\right)(\Delta PS)^{1/2} \tag{1}$$

h_t	enthalpy total, Btu/lbm
KR	Visco Jet outlet indicator: if 1, then saturated outlet; if 2, then subcooled outlet
Lohm	Lohm rating, 1 Lohm = 100 g/min H_2O per 25 psid at 80 °F
MDATA	measured flow rate, lbm/hr
MLEE	calculated flow rate with Lee equation, lbm/hr
MMOD	calculated flow rate with modified Lee equation, lbm/hr
$\dot{m}$	calculated mass flow rate, lbm/hr
PIN	inlet pressure to Visco Jet, psia
POUT	outlet pressure of Visco Jet, psia
S	specific gravity: Visco Jet inlet density, $(lbm/ft^3)/62.4$
TIN	inlet temperature to Visco Jet, °R
TOUT	outlet temperature of Visco Jet, °R
TSAT	saturation temperature at PIN, °R
X	quality
x	independent parameter in analytical model
ΔP	pressure difference across the Visco Jet, psid

EXPERIMENTAL EQUIPMENT

The Visco Jet Test Apparatus is designed as a test stand mounted on a wheeled cart to enable a high degree of flexibility within the test program. It can flow either liquid nitrogen or liquid hydrogen without modification. A design goal was the minimization of heat leak into the test article to maintain the flow process as close to isenthalpic as possible.

Flow System

Figure 1 is a system schematic of the Visco Jet Test Stand showing the mobile 250 gal liquid nitrogen supply dewar connected to the test rig through a vacuum jacketed fill line. The cylindrical vacuum chamber which houses the Visco Jet as part of the flow system is 10 in. in diameter with a height of 19 in. The entire rig, including the test chamber and the flow system piping, is made of stainless steel. The fluid transfer line and the inlet piping to the test chamber flange are vacuum jacketed. The liquid flow control valve between the supply dewar and the test chamber is also vacuum jacketed and pneumatically actuated. Pressure regulating valves downstream of the flow system

piping are also pneumatically actuated but not vacuum jacketed. Vapor vent on/off valves for routing the flow through a bank of flow meters are controlled by solenoid valves that are housed within a nitrogen-purged box.

There are two Visco Jets mounted within the test chamber. The one labeled primary is the test article while the other labeled secondary is part of a heat exchanger system. Liquid nitrogen from the supply dewar enters the test chamber flow system through a flange feed through port and flows in an upward direction where it is divided into three parts by a cross in the line. The test fluid that flows through the primary Visco Jet turns into downward flow where it traverses the heat exchanger, an electrically heated coil, the primary Visco Jet, the vapor trap coil, the air heat exchanger, a bank of flowmeters and finally discharges through an air ejector to the vent system. The heater coil between the heat exchanger and the primary Visco Jet is used to raise the fluid temperature, while the secondary Visco Jet discharging through the heat exchanger is used to cool the inlet test fluid. By selectively using the heat exchanger and the heater coil, it is possible to condition the test fluid to cover a wide range of inlet temperatures from high subcooling to near saturated inlet conditions. The vapor trap coil, downstream of the primary Visco jet, is installed to prevent buoyancy driven vapor, located outside the vacuum tank, from coming up the tube to the temperature measuring station, downstream of the primary Visco Jet.

The test fluid that flows downstream of the Visco Jet is completely vaporized in an air heat exchanger prior to its passage through a bank of gas flow meters discharging through an atmospheric vent. The primary ejector pump, between the flow meters and the vent, is operated to reduce the line pressure below 1 atm to simulate low vacuum space conditions.

The cross in the line diverts some of the fluid through the secondary Visco Jet to the outer flow passage of the double tube type heat exchanger, and then discharges through the secondary air ejector to the vent system. The balance of the fluid separated from the inlet flow by the cross in the line, labeled bypass flow in figure 1, enters the coils of the cold wall and discharges to the atmosphere. Figure 2 is a photograph of the exterior view of the cold wall showing the coils brazed to the wall itself. The wall is essentially a thin stainless shell surrounded by an aluminized mylar thermal shield (not shown) to reduce radiation from the test chamber wall to the cold wall. A nominal bypass flow rate was determined during initial operations based on maintaining a constant cold wall temperature.

A photograph of the plumbing within the test chamber with the cold wall removed is shown in figure 3. The lines made of 1/4-in. seamless tubing with a 0.28 wall thickness are shaped to relieve stress during thermal cycling.

Test Article

The Joule-Thomson device (Visco Jet) used in this study is essentially a group of orifices in series encapsulated in a fitting for installation within a flow system. Figure 4 taken from the Lee Technical Hydraulic Handbook (ref. 2) is a schematic of the orifice arrangement within a disc. The resistance to flow is generated by complex flow passages between a series of these discs containing spin chambers mounted in the fitting perpendicular to flow. The fluid

changes direction many times resulting in a pressure drop much greater than would be obtained with a normal metering hole of the same diameter.

Four sets of Visco Jets, with different Lohm ratings each, were purchased from the Lee Company. Each set consisted of six individual Visco Jet units of similar Lohm rating. Each Visco Jet was calibrated with water and the results checked against the nominal Lohm ratings supplied by the manufacturers. Table I lists the manufacturer's specified and the calibrated Lohm ratings for each test article. Although differences varied as much as 11 percent, the Visco Jets chosen for this study, as noted in the table, are within ±3.5 percent of the nominal values.

Instrumentation

The flow system schematic of the Visco Jet test apparatus (fig. 1) shows the location of the instrumentation. Within the vacuum chamber, fluid pressure and temperature measurements were obtained upstream and downstream of the primary Visco Jet under test. Additional temperature measurements were made of the primary Visco Jet body and the bypass fluid. Temperature and pressure measurements were also made within the support, plumbing upstream and downstream the bank of flow meters to assure their operation within design specifications. The pressure measurements were made with strain gage type transducers and temperature measurements with silicon diode sensors. Instrumentation calibrations were made prior to the initial data runs and after the testing was completed. During the testing, continuous checks were made by comparing the outputs of instruments that were under identical test conditions.

Mass flow rates of the test fluid through the primary Visco Jet, after warming to ambient conditions, were measured by a bank of four thermal conductivity type flow meters. Because of the wide range of flows required for testing, each flow meter covered a specific range of flows. The flow meter used for a particular test was selected by valving to maintain the readings within its operating range.

Data Acquisition System

The Visco Jet test stand, mounted on a moveable cart along with valves, plumbing and flow meters, was stationed within a test cell. Remote operation of the rig was achieved through a control panel located in the control room. The data acquisition system was an analog-to-digital multiplexor connected to a dedicated personal computer (PC). The multiplexor received voltage signals from the test rig that were then digitized and converted to integer counts. A computer code then converted the counts to engineering units for data manipulation. Online test conditions were displayed in engineering units on the PC monitor and the data was stored on the PC's hard disc. The data stored in this manner was then transferred to a floppy disc for processing.

EXPERIMENTAL PROCEDURE

Prior to testing, the chamber housing the Visco Jet was evacuated to about 35 μm of mercury at which time the vacuum pump was isolated from the rig. The integrity of the vacuum system was established by noting an insignificant gain

in pressure over a 24-hr time interval. The vacuum was continuously monitored with a vacuum gage during the testing. After the integrity of the vacuum system was established, the system piping was purged with gaseous helium to eliminate water vapor and air from the system. The liquid nitrogen supply dewar was then pressurized by nitrogen boil-off through an external vaporizer to a pressure above that required for the test. Chilldown of the entire test rig was achieved by flowing liquid nitrogen through the system piping.

The controlled parameters for setting up test conditions were inlet and exit Visco Jet pressures, inlet Visco Jet temperature, and bypass flow. A typical data run consisted of establishing a fixed inlet pressure and temperature upstream of the Visco Jet and then varying the downstream pressure. A data point was recorded at discrete exit pressure levels for 30 readings at 5-sec intervals for averaging and to establish the steady-state nature of the flow.

Data were obtained over a range of inlet pressures from 30 to 60 psia, inlet temperatures from 118 to 164 °R, outlet pressures from 2.8 to 55.8 psia, outlet temperatures from 117 to 162 °R, and flow rates from 0.04 to 4.0 lbm/hr of nitrogen. All the basic data are listed in tables II(a) to (d) for Visco Jets with flow resistances represented by Lohm ratings of 17 000, 41 000, 80 000, and 243 000, respectively.

DATA PRESENTATION

Four sets of liquid nitrogen mass flow data, as a function of pressure drop across the Visco Jets, are presented in figures 5(a) to (d). Each succeeding figure from a to d is for Visco Jets with increasing resistance to flow. The data for the Visco Jet with the least resistance to flow having a Lohm rating of 17 600 is shown in figure 5(a). The various symbols on the plot identify seven data runs at three different inlet pressures. The 60 psia data includes five data runs at inlet temperatures from 120 to 162 °R that cover a wide range of inlet subcooling, up to near-saturated inlet conditions. In contrast, the 45 and 30 psia data are limited to near saturated inlet conditions. The region between the two lines on the plot represents the locus of the Lee equation from reference 2 that predicts noncavitating liquid flow through the Visco Jets. The 5 percent spread in the band is caused by fluid density differences at inlet conditions (i.e., 120 to 162 °R). It is apparent that a good percentage of the data represented by a square, a circle, a diamond, and an upright triangle falls between these two lines.

For fluid inlet conditions of 60 psia and 120 °R representing relatively high inlet subcooling, the open squared data follows the Lee equation over most of the range of pressure differences across the Visco Jet. However, as the subcooling is decreased by raising the inlet temperature to 129 °R, a departure from the Lee equation is noted by a drop in the flow rate above a pressure difference of 50 psid. Further decreases in subcooling, as noted by increasing the inlet temperature to 148 °R, move the departure point to even lower values of pressure drop. At near-saturated inlet conditions of 162 °R, the decrease in flow rate from that predicted by the Lee equation occurs at a pressure drop of 5 psid. Both the 45 and 30 psia data at near-saturated inlet conditions also drop off at about the same pressure differences.

An additional data trend noted in figure 5(a) is the absence of an inlet pressure effect on the near-saturated inlet data. All three near-saturated

inlet data runs at inlet pressures of 60, 45, and 30 psia fall along the same curve. An examination of the basic data in table II will show that the decrease in flow from that predicted by the Lee equation coincides with downstream fluid temperatures equal to saturation values based on downstream pressures. Consequently, the higher the inlet subcooling, the more pressure drop is required to obtain cooling via the Joule-Thomson effect.

The data trends noted in figure 5(a) for a Visco Jet with a Lohm rating of 17 600 are again noted in figure 5(b) for a Visco Jet with a Lohm rating of 41 000. The most significant difference is the 50 percent reduction in flow rate due to the increased resistance to flow.

Figure 5(c) presents the data for a Visco Jet with a Lohm rating of 80 000. The trends in the data are again similar to the trends in the figure 5(b) 41 000 Lohm Visco Jet data. Again, the most significant difference is the level of the flow rate data that drops off about 50 percent more due to increased resistance to flow.

The fourth set of data (fig. 5(d)) was obtained with a Visco Jet having a 243 000 Lohm rating. The increased resistance to flow over the figure 5(c) 80 000 Lohm Visco Jet data results in an additional 70 percent drop in the flow rate. Although the data trends for all four sets of data are similar, the flow rate measurement for this set of data appears to be high. The Lee equation for liquid flow underpredicts the single-phase flow by about 8 percent. An increased amount of uncertainty exists for this particular set of data due to the extremely low flow rate measurements which most likely contribute to the offset and increased scatter in the data.

DATA CORRELATION AND DISCUSSION

The spread of the basic data in figures 5(a) to (d) shows that the Lee equation adequately predicts a portion of the data and overpredicts the balance of the data by as much as 30 percent. In order to clearly show these differences, the basic measured flow data were plotted versus the flow rates obtained from the Lee equation. An examination of figure 6, which presents the 41 000 Lohm rating Visco Jet data, shows the data divided into two categories of exit flow conditions. The data shown as a circle falls along the solid line that represents agreement between the data and the Lee equation for noncavitating flow (single phase). The data shown as a square, that falls as much as 28 percent off the line, represents cavitating flow (two-phase) exit conditions.

The thermodynamic state of the outlet flow is determined by comparing the fluid enthalpies across the Visco Jet. If the inlet enthalpy is greater than the saturated liquid enthalpy at the outlet pressure, then quality exists in the outlet flow. The exit thermodynamic state of the fluid is identified in column KR of table II for all the data runs. When KR = 1, the outlet fluid is at saturated conditions and two-phase flow can exist. When KR = 2, the outlet fluid is subcooled and only single-phase flow exists.

Isenthalpic expansion calculations were then made for all the two-phase data to determine the extent of quality available in the exit flow by using the following equation:

$$h_t = Xh_g + (1 - X)h_l \tag{2}$$

where h_t is the inlet enthalpy, and h_g and h_l are the saturated gas and liquid enthalpies at the outlet pressure, respectively. The results of the calculations are presented in column X of table II.

The correlation procedure reported herein is based on a reduction in the mass flux during a phase change within the body of the multiple orifice Visco Jet. Because the quality reduces the average density of the fluid in the flow passage, it is directly related to the reduction in flow rate. Since the mass fraction of liquid in a two-phase system is equal to one minus the quality, a term equal to 1 - X was used to identify the change in flow rate. The Lee equation which has been shown to adequately predict liquid nitrogen single-phase flow was then modified by a multiplication factor equal to 1 - X to attempt to reduce the spread in the figure 6 data. The completed data correlation follows:

$$\dot{m} = \left(\frac{10\ 000}{\text{Lohm}}\right)(\Delta PS)^{1/2}(1 - X) \tag{3}$$

The result of the modification, presented in figure 7, shows a marked improvement in the data correlation. Most of this particular set of data falls within a 10 percent error band.

All four sets of Visco Jet data are plotted in figure 8 as experimental mass flow versus predicted mass flow using the modified Lee equation. The data, covering a wide range of flow rates, is divided by the vertical lines on the plot into four groupings. Each group identifies the range of flow covered by each Visco Jet with some overlap. The solid lines, encompassing a great deal of the data, represent a ±10 percent scatter band from perfect agreement. Again, single- and two-phase data are identified by an open circle and an open square, respectively. It is significant to note that almost all the single-phase data fall within the 10 percent scatter band except for two data points in the extremely low flow rate region. The balance of the single-phase data in this region is also high compared to the other three sets of single-phase data suggesting some additional uncertainty in the data measurements, possibly due to the extremely low flow rate measurements. Although the absolute error is comparable for all sets of data, the percent error is much larger in the low flow rate region. In addition, the two-phase data in this low flow rate region also appears high.

At the opposite end of the plot the data represented by a solid square, obtained with the 17 600 Lohm rating Visco Jet, falls significantly outside of the 10 percent scatter band. This data, obtained consecutively at the end of a test run, is thought to be erroneous due to the phenomenon of partial blockage within the Visco Jet. The suspect data is identified as such in the tabulated basic data. Partial blockage also occurred on two other occasions with different Visco Jets during data acquisition. For these cases, the problem was identified at the time and the runs were repeated after allowing the rig to warm up to ambient conditions. The blockage phenomenon is tentatively attributed to freeze up trace liquid contaminates in the test fluid. When blockage became apparent during data acquisition, the test rig would be allowed to warm up to ambient conditions, thus allowing the contaminates to thaw and pass through the Visco Jet.

An examination of the reliable data in figure 8, covering a range of Visco Jet Lohm ratings between 17 600 to 80 000, shows that 100 percent of the single-phase data and 85 percent of the two-phase data fall within the ±10 percent scatter band. An attempt should be made during the remainder of the test program to reduce the scatter in the data correlation and to extend the range of correlated Visco Jet Lohm ratings. In addition, an attempt should be made to positively identify the cause of flow blockage within the body of the Visco Jet and evaluate solutions for its prevention.

SUMMARY OF RESULTS

A test rig was constructed capable of obtaining liquid hydrogen and liquid nitrogen flow rate, pressure drop, and temperature drop data across a series of four Visco Jets with flow resistances represented by Lohm ratings of 17 000, 41 000, 80 000, and 243 000. The liquid nitrogen results are reported herein. The data includes a range of inlet pressures from 30 to 60 psia, inlet temperatures from 118 to 164 °R, outlet pressures from 2.8 to 55.8 psia, outlet temperatures from 117 to 162 °R and flow rates from 0.04 to 4.0 lbm/hr.

The data were applied to the Lee equation supplied by the Visco Jet manufacturer that predicts hydraulic fluids flow rates with the following results:

1. For fluid resistances identified by Visco Jet Lohm ratings from 17 600 to 80 000, the Lee equation was found to predict 100 percent of the single-phase liquid nitrogen data within ±10 percent accuracy, but overpredicted the two-phase data by as much as 30 percent.

2. A two-phase data correlation scheme was developed based on the generation of vapor within the body of the Visco Jet that results in a reduction in flow rate. The Lee equation, modified with a multiplication term equal to one minus the quality based on an isenthalpic expansion, predicts 85 percent of the reliable two-phase data within ±10 percent accuracy for Visco Jet Lohm ratings from 17 600 to 80000.

3. The extremely low flow rate data obtained with the 24 300 Lohm rating Visco Jet was not included in the percent scatter evaluation because of increased data uncertainty and larger percentage errors in measurements at low flow rates.

4. Suggestions are made for a continuation of the test program to reduce the scatter in the data correlation and to further investigate the phenomenon of partial flow blockage within the body of the Visco Jet that occurred several times during the data runs.

APPENDIX - Error Analysis

The comparison of experimental data with theory is valid only when all the errors in the measurements and predicted calculations are considered. The value that a device measures can deviate from the true value of the measurement due to experimental errors. Examples of such errors are the signal errors (transducer, signal conditioner, amplifier, recorder), sensitivity drift, operation of device beyond its normal range, electronic noise, human error, etc. Therefore, in order to have confidence in the measured value, a range within which the true value may exist (device accuracy) is determined by calibrating the device. In this experiment these errors were as follows. The accuracies of absolute pressure measurements across the Visco Jet were ±1 percent of full scale value (100 psia), ±1.8 °R for temperature measurements, and ±1 percent of full scale for the flow meters downstream of the Visco Jet. The flow meter range for the 17 600, 41 000 and 80 000 Lohm Visco Jets was 0 to 7.5 lbm/hr and for 243 000 Lohm Visco Jet was 0 to 0.75 lbm/hr.

The uncertainty in the predicted calculations is referred to as analytical model accuracy. While the errors due to signal conditioning, drift, etc. accumulate to become device accuracy, the uncertainties in the input parameters to the theoretical model such as pressure, temperature, etc. accumulate to become analytical model accuracies. A widely accepted method of determining the model accuracy ℓ_F is given in reference 3 as

$$\ell_F = \left[(\ell_{x1}F_{x1})^2 + (\ell_{x2}F_{x2})^2 + (\ell_{x3}F_{x3})^2 + \ldots + (\ell_{xn}F_{xn})^2\right]^{1/2} \tag{4}$$

where $F = F(x_1, x_2, x_3, \ldots, x_n)$ the analytical model with n independent parameters. F_x is the partial derivative of F with respect to input parameter x. The approach was applied to the semiempirical model used for the analysis in this experiment (eq. (3)). It showed that the errors in absolute pressures were minute in relation to the ±3.5 percent error in the Lohm rating. Consequently, the analytical model accuracy was nearly identical to the percentage error in the Lohm rating.

Once all the accuracies are determined, the following technique is used to compare the predicted values to the experimental values. The ordinate of a graph is labeled as experimental value and the abscissa as the predicted value. A line with a slope of 1 is drawn covering the full range of the graph. The experimental and predicted values are graphed as well as their uncertainty values. For a given experimental and predicted point on the graph, the uncertainty in the experimental value gives a vertical line, whereas the uncertainty in the predicted value gives a horizontal line through the point. A box whose boundary coincides with the ends of the two lines is drawn around the graphed point. The box indicates the region where the true graphed point exists due to the device and the analytical model accuracies. The shape of the box compares the relative magnitude of the experimental to predicted errors. If the box is a square, then the errors are numerically identical. If rectangle, however, then the axis parallel to its length contributes more toward the total error than the perpendicular axis. Once all the boxes are drawn, the theoretical model is determined as validated if the line with a slope of 1 crosses the boxes at any location. The indication to modify the predicted model is evident if most of the boxes are to either the right or left side of the line. If

most of the boxes are to the right, then the modification should be to reduce the predicted values and vice versa.

The results of this technique when applied to the current experiment are shown in figure 9 for 41 000 Lohm. The solid circle indicates the data point if there were no errors present and the box is explained above. As indicated, the predicted errors are slightly less than the experimental errors. The line slope of 1 crosses the majority of the boxes, thus indicating the validity of the modified Lee equation within experimental and theoretical errors.

REFERENCES

1. Anderson J.E.; and Eberhardt, R.N.: Cryogenic Storage System Development For Long Term Space Missions. AIAA/SAE/ASME Joint Propulsion Conference, 15th, AIAA, New York, 1979, paper No. 79-1261.

2. Technical Hydraulic Handbook. Seventh edition, Lee Company, Westbrook, CT, 1984.

3. Holman J.P.: Experimental Methods for Engineers. Fourth edition, McGraw Hill, 1984.

TABLE I. - VISCO JET WATER CALIBRATION TEST RESULTS

Lohm rating	Unit	Flow rate, lbm/hr	Calculated Lohm	Percent error
17 600	1	2.948	16 950	-3.70
	2	2.672	18 700	6.24
	[a]3	2.864	17 440	-0.88
	4	2.896	17 250	-1.98
	5	2.908	17 180	-2.38
	6	2.938	17 000	-3.38
41 000	1	1.174	42 560	3.80
	2	1.160	43 070	5.05
	[a]3	1.218	41 020	0.05
	4	1.216	41 090	0.21
	5	1.176	42 480	3.60
	[a]6	1.182	42 270	3.10
80 000	1	.604	82 640	3.30
	2	.574	86 960	8.70
	[a]3	.610	81 830	2.28
	4	.582	85 760	7.21
	5	.604	82 640	3.30
	6	.562	88 820	11.00
243 000	1	.194	257 500	5.98
	2	.198	252 300	3.84
	3	.198	252 300	3.84
	4	.198	252 300	3.84
	5	.196	254 900	4.90
	[a]6	.200	249 800	2.80

[a]Data obtained with these Visco Jets.

TABLE II. - VISCO JET DATA

(a) 17 600 Lohm

ΔP	MDATA	MMOD	MLEE	PIN	POUT	TIN	TOUT	TSAT	X	KR
56.00	3.33	3.42	3.82	59.08	3.08	138.25	118.36	164.65	0.1046	1
50.86	3.28	3.46	3.64	58.29	7.42	138.07	128.63	164.36	.0486	1
44.13	3.14	3.39	3.39	58.19	14.06	138.10	138.08	164.33	.0000	2
29.86	2.61	2.79	2.79	57.54	27.68	138.04	138.59	164.08	.0000	2
18.68	2.12	2.21	2.21	57.58	38.91	138.07	138.53	164.10	.0000	2
9.74	1.52	1.59	1.59	56.67	46.93	138.06	138.30	163.75	.0000	2
15.53	1.96	2.04	2.04	62.41	46.88	128.57	128.72	165.85	.0000	2
22.82	2.36	2.47	2.47	62.25	39.43	129.40	129.96	165.80	.0000	2
32.83	2.78	2.96	2.96	61.73	28.90	129.90	130.36	165.61	.0000	2
42.95	3.21	3.39	3.39	57.23	14.28	129.78	130.37	163.97	.0000	2
53.56	3.57	3.77	3.78	60.99	7.43	129.96	128.65	165.35	.0033	1
54.45	3.49	3.65	3.81	58.75	4.30	130.26	122.04	164.53	.0418	1
57.72	3.56	3.70	3.93	60.83	3.11	129.70	118.85	165.29	.0579	1
57.32	3.81	3.89	3.96	60.49	3.17	122.22	118.89	165.17	.0164	1
52.38	3.60	3.78	3.78	59.57	7.19	121.85	122.77	164.83	.0000	2
41.75	3.22	3.38	3.38	57.23	15.47	121.44	122.19	163.97	.0000	2
28.48	2.77	2.80	2.80	56.23	27.76	120.41	120.95	163.59	.0000	2
15.97	2.11	2.10	2.10	55.47	39.51	119.55	120.20	163.30	.0000	2
8.99	1.55	1.57	1.57	59.10	50.11	120.79	121.26	164.66	.0000	2
55.40	3.09	3.14	3.74	58.35	2.95	148.13	118.20	164.38	.1596	1
50.29	3.04	3.20	3.56	57.94	7.64	148.19	128.70	164.23	.1025	1
43.11	2.96	3.15	3.30	57.44	14.32	147.09	137.75	164.05	.0480	1
28.06	2.52	2.66	2.66	56.64	28.59	147.49	147.72	163.74	.0000	2
19.54	2.10	2.22	2.22	58.27	38.74	147.98	148.19	164.35	.0000	2
9.48	1.47	1.55	1.55	57.72	48.24	148.62	148.66	164.15	.0000	2
[a]9.17	1.20	1.46	1.48	57.29	48.12	162.77	159.07	163.99	.0156	1
17.87	1.51	1.99	2.07	56.72	38.85	162.58	154.83	163.77	.0404	1
29.87	1.77	2.46	2.67	57.08	27.20	162.78	148.14	163.91	.0799	1
42.17	2.01	2.74	3.18	56.45	14.28	162.64	137.83	163.67	.1366	1
48.93	2.05	2.79	3.42	56.24	7.31	162.47	128.26	163.59	.1840	1
53.57	2.18	2.72	3.58	56.18	2.61	162.49	116.77	163.57	.2419	1
42.79	2.01	2.53	3.23	45.33	2.54	157.70	116.37	159.10	.2175	1
37.38	1.85	2.57	3.02	45.20	7.82	157.25	128.73	159.04	.1504	1
30.86	1.78	2.45	2.75	45.12	14.26	157.30	137.70	159.00	.1060	1
17.42	1.45	1.97	2.06	44.91	27.50	157.30	148.28	158.91	.0460	1
5.00	.92	1.10	1.10	44.93	39.93	157.38	155.24	158.92	.0050	1
3.26	.72	.90	.90	30.83	27.57	150.55	148.29	151.67	.0054	1
10.35	1.11	1.56	1.61	31.70	21.35	150.74	143.88	152.18	.0323	1
17.04	1.36	1.92	2.06	31.28	14.25	150.63	137.69	151.93	.0680	1
23.91	1.52	2.16	2.45	31.36	7.45	150.55	128.31	151.98	.1166	1

[a]The following three sets of data are with partially blocked Visco Jet.

TABLE II. - Continued

(b) 41 000 Lohm

ΔP	MDATA	MMOD	MLEE	PIN	POUT	TIN	TOUT	TSAT	X	KR
54.41	1.52	1.54	1.64	57.51	3.10	130.25	118.97	164.07	0.0610	1
50.03	1.53	1.57	1.57	57.53	7.50	129.62	130.28	164.08	.0006	1
43.01	1.39	1.46	1.46	57.55	14.54	129.02	129.46	164.09	.0000	2
29.91	1.19	1.21	1.21	57.48	27.56	130.32	130.50	164.06	.0000	2
18.31	.95	.95	.95	57.50	39.19	130.00	130.33	164.07	.0000	2
13.70	.81	.82	.82	59.04	45.34	130.30	130.51	164.64	.0000	2
14.07	.80	.82	.82	60.83	46.76	138.32	138.61	165.29	.0000	2
23.15	.99	1.05	1.05	62.38	39.22	138.48	138.62	165.84	.0000	2
34.63	1.23	1.29	1.29	62.25	27.61	138.60	138.61	165.80	.0000	2
47.98	1.44	1.52	1.52	62.56	14.58	138.57	138.68	165.91	.0000	2
56.72	1.54	1.56	1.65	64.07	7.35	138.54	138.68	166.43	.0520	1
58.61	1.53	1.50	1.68	61.76	3.15	138.23	118.74	165.62	.1033	1
55.55	1.38	1.35	1.61	58.57	3.03	148.02	118.35	164.47	.1576	1
50.14	1.31	1.37	1.53	57.77	7.62	148.15	129.06	164.17	.1024	1
43.65	1.26	1.35	1.42	58.20	14.56	148.34	138.24	164.33	.0537	1
30.00	1.13	1.18	1.18	57.47	27.46	148.03	148.31	164.06	.0000	2
18.70	.91	.93	.93	57.22	38.52	147.96	148.40	163.96	.0000	2
9.15	.66	.65	.65	56.78	47.63	147.51	148.39	163.80	.0000	2
55.09	1.14	1.18	1.56	57.97	2.89	163.27	117.61	164.24	.2411	1
50.40	1.09	1.21	1.49	57.92	7.53	163.39	129.06	164.22	.1872	1
42.14	1.02	1.18	1.36	57.10	14.96	162.91	138.61	163.92	.1344	1
33.30	1.00	1.12	1.21	60.00	26.70	162.20	148.12	164.99	.0784	1
18.78	.76	.87	.91	59.16	40.38	163.89	155.77	164.68	.0441	1
10.51	.68	.66	.68	58.25	47.74	163.61	163.64	164.35	.0219	1
9.94	.60	.65	.67	45.00	35.06	158.52	153.19	158.95	.0271	1
15.88	.72	.81	.84	44.33	28.45	157.83	149.20	158.65	.0456	1
29.38	.85	1.03	1.15	44.07	14.69	157.62	138.58	158.53	.1054	1
37.21	.89	1.09	1.29	44.40	7.19	157.45	128.46	158.68	.1571	1
41.04	1.01	1.07	1.36	43.84	2.80	157.14	117.35	158.42	.2097	1
29.54	.88	.95	1.16	32.25	2.71	151.60	117.12	152.50	.1818	1
24.97	.81	.94	1.07	32.49	7.53	151.72	129.05	152.64	.1223	1
16.49	.70	.81	.87	31.10	14.61	150.85	138.32	151.83	.0671	1
9.43	.58	.64	.66	30.67	21.24	150.55	144.21	151.57	.0317	1
4.19	.41	.43	.44	31.58	27.39	151.39	148.55	152.11	.0111	1

TABLE II. - Continued

(c) 80 000 Lohm

ΔP	MDATA	MMOD	MLEE	PIN	POUT	TIN	TOUT	TSAT	X	KR
58.02	0.85	0.84	0.87	60.87	2.84	124.92	117.54	165.30	0.0372	1
57.18	.87	.86	.87	59.95	2.77	120.67	117.50	164.97	.0158	1
52.33	.82	.83	.83	59.84	7.51	120.46	121.20	164.93	.0000	2
46.39	.82	.79	.79	60.68	14.29	119.20	119.34	165.24	.0000	2
32.93	.65	.66	.66	60.75	27.82	121.40	121.42	165.26	.0000	2
23.95	.56	.57	.57	60.79	36.84	119.09	120.09	165.28	.0000	2
13.41	.42	.42	.42	60.71	47.30	118.43	119.34	165.25	.0000	2
12.44	.39	.40	.40	60.88	48.44	128.94	129.12	165.31	.0000	2
23.73	.54	.55	.55	60.91	37.18	128.75	129.43	165.32	.0000	2
33.33	.64	.66	.66	60.84	27.51	128.71	129.42	165.29	.0000	2
45.97	.76	.77	.77	60.67	14.69	128.68	129.07	165.23	.0000	2
53.43	.80	.83	.83	60.89	7.46	129.43	130.01	165.31	.0001	1
58.09	.84	.81	.87	60.81	2.72	130.55	131.15	165.28	.0699	1
58.08	.82	.76	.86	60.76	2.68	137.84	116.90	165.27	.1099	1
52.81	.77	.78	.82	60.46	7.64	138.34	129.10	165.16	.0481	1
45.88	.68	.76	.76	60.30	14.42	138.56	138.23	165.10	.0000	2
32.04	.59	.64	.64	60.56	28.51	138.60	139.16	165.19	.0000	2
22.94	.51	.54	.54	60.53	37.59	138.60	139.29	165.18	.0000	2
11.87	.37	.39	.39	60.19	48.32	138.83	139.66	165.06	.0000	2
56.77	.75	.70	.83	59.37	2.60	146.61	116.67	164.76	.1581	1
51.78	.69	.71	.80	59.23	7.45	148.09	128.98	164.71	.1037	1
44.73	.69	.70	.74	59.08	14.35	147.99	138.22	164.65	.0530	1
29.29	.55	.60	.60	60.17	30.88	148.14	148.05	165.05	.0000	2
19.39	.45	.49	.49	59.67	40.28	148.16	148.93	164.87	.0000	2
11.70	.36	.38	.38	59.57	47.87	147.41	149.14	164.83	.0000	2
11.47	.31	.36	.36	59.64	48.17	162.28	159.25	164.86	.0124	1
20.52	.40	.46	.49	59.03	38.50	163.84	154.80	164.64	.0493	1
30.58	.48	.55	.59	58.68	28.10	163.62	148.99	164.51	.0817	1
44.39	.59	.62	.72	58.83	14.44	163.20	138.20	164.56	.1390	1
50.22	.61	.62	.76	58.20	7.98	163.11	129.58	164.33	.1818	1
55.55	.65	.60	.80	58.09	2.54	163.00	116.40	164.29	.2459	1
43.62	.59	.56	.72	46.12	2.50	158.23	116.25	159.45	.2211	1
38.27	.51	.57	.67	46.00	7.73	158.23	129.28	159.40	.1566	1
31.97	.49	.54	.61	46.31	14.34	158.55	138.19	159.53	.1127	1
18.38	.39	.44	.47	45.82	27.44	157.88	148.51	159.32	.0496	1
6.49	.28	.27	.28	45.68	39.19	157.90	155.03	159.25	.0105	1
6.09	.24	.27	.27	33.78	27.68	152.32	148.84	153.36	.0155	1
17.97	.40	.45	.47	37.18	19.22	148.51	142.54	155.19	.0295	1
21.86	.43	.48	.52	36.29	14.43	149.74	138.23	154.72	.0620	1
26.43	.47	.50	.56	33.70	7.27	151.46	128.53	153.32	.1233	1
29.56	.49	.49	.60	32.01	2.44	150.96	115.81	152.36	.1836	1

TABLE II. - Concluded

(d) 243 000 Lohm

ΔP	MDATA	MMOD	MLEE	PIN	POUT	TIN	TOUT	TSAT	X	KR
56.04	0.31	0.28	0.28	59.09	3.05	123.30	118.44	164.66	0.0244	1
56.00	.29	.28	.28	58.98	2.98	118.94	118.01	164.62	.0024	1
49.98	.28	.27	.27	57.51	7.53	118.07	120.08	164.07	.0000	2
43.53	.26	.25	.25	57.91	14.38	117.90	119.38	164.22	.0000	2
31.12	.23	.21	.21	59.25	28.13	118.22	120.06	164.72	.0000	2
17.06	.16	.16	.16	58.48	41.42	119.15	121.31	164.43	.0000	2
8.04	.12	.11	.11	57.26	49.21	119.48	122.34	163.98	.0000	2
10.88	.13	.12	.12	58.58	47.70	138.37	138.52	164.47	.0000	2
18.64	.17	.16	.16	57.76	39.12	138.71	139.99	164.16	.0000	2
30.75	.21	.20	.20	58.00	27.25	138.72	140.40	164.25	.0000	2
44.18	.25	.25	.25	58.64	14.46	138.60	139.98	164.49	.0000	2
50.87	.27	.25	.26	58.60	7.73	138.23	129.06	164.48	.0466	1
53.64	.28	.25	.27	57.65	4.01	137.82	120.97	164.12	.0872	1
56.52	.29	.25	.28	59.46	2.94	137.69	117.55	164.79	.1041	1
56.59	.28	.23	.27	59.60	3.00	148.49	117.79	164.84	.1607	1
50.85	.26	.23	.26	58.84	7.99	150.32	129.37	164.57	.1111	1
43.72	.24	.23	.24	58.11	14.39	148.75	137.70	164.30	.0570	1
31.81	.20	.21	.21	59.77	27.95	148.06	145.62	164.91	.0000	2
19.97	.17	.16	.16	58.26	38.29	147.58	149.02	164.35	.0000	2
9.03	.11	.11	.11	58.75	49.72	150.41	148.61	164.53	.0000	2
1.90	.06	.05	.05	58.79	56.90	148.92	150.55	164.55	.0000	2
54.53	.26	.20	.26	57.45	2.92	161.51	117.55	164.05	.2311	1
51.25	.25	.21	.25	58.74	7.49	162.28	128.64	164.53	.1814	1
44.50	.24	.20	.24	58.89	14.39	162.38	137.71	164.58	.1345	1
31.57	.20	.18	.20	58.80	27.23	162.64	148.10	164.55	.0790	1
20.25	.15	.15	.16	58.48	38.23	162.55	154.35	164.43	.0421	1
9.11	.12	.11	.11	58.74	49.63	160.75	156.90	164.53	.0000	2
2.15	.06	.05	.05	58.17	56.02	162.21	158.67	164.32	.0000	2
43.00	.22	.18	.23	45.76	2.76	157.57	117.44	159.29	.2128	1
38.69	.21	.19	.22	46.16	7.46	157.69	129.04	159.47	.1560	1
32.07	.19	.18	.20	46.41	14.34	157.84	138.23	159.58	.1087	1
16.51	.13	.14	.15	46.09	29.58	157.93	150.04	159.44	.0421	1
6.20	.10	.09	.09	45.80	39.60	157.51	153.22	159.31	.0069	1
2.22	.06	.05	.05	45.82	43.60	158.21	156.22	159.32	.0000	2
29.87	.19	.16	.20	32.55	2.69	151.54	116.90	152.67	.1819	1
22.87	.16	.15	.17	30.74	7.87	149.94	129.54	151.61	.1094	1
17.73	.14	.14	.15	32.06	14.33	150.88	138.21	152.39	.0689	1
9.93	.11	.11	.11	31.97	22.03	150.87	144.95	152.34	.0301	1
4.70	.13	.08	.08	30.94	26.24	150.49	147.74	151.73	.0103	1
1.26	.05	.04	.04	32.55	31.28	151.74	149.74	152.67	.0000	2

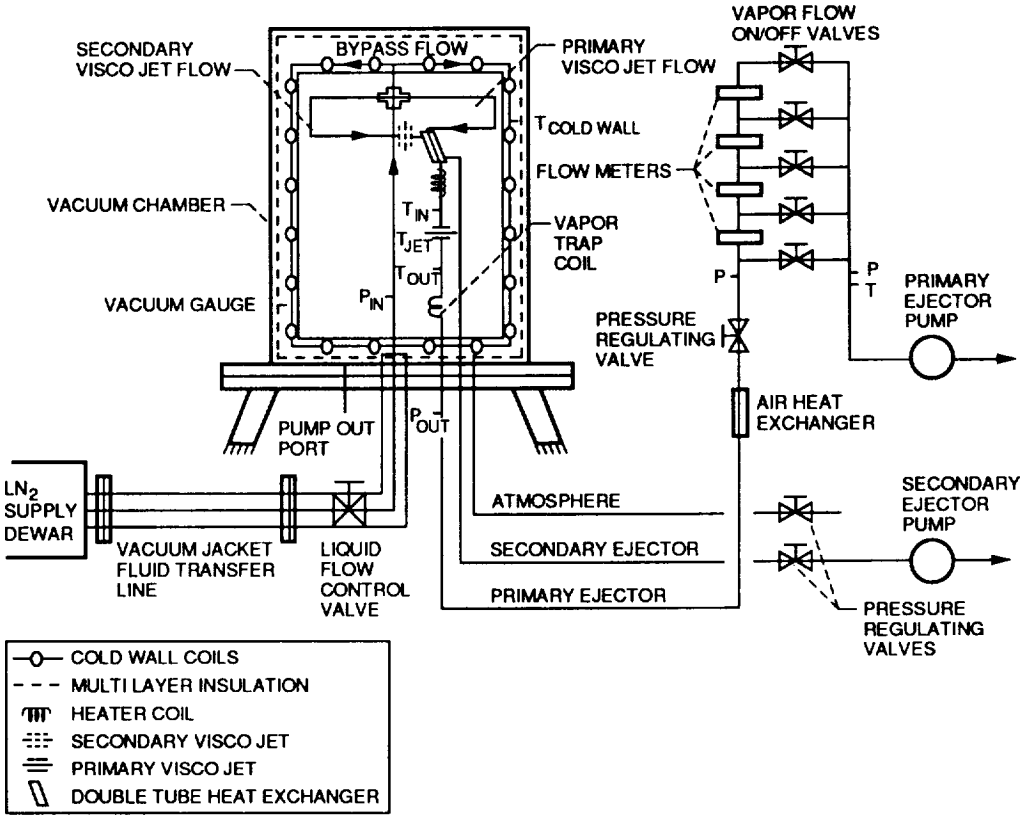

Figure 1. - Joule-Thomson device test rig schematic.

ORIGINAL PAGE
BLACK AND WHITE PHOTOGRAPH

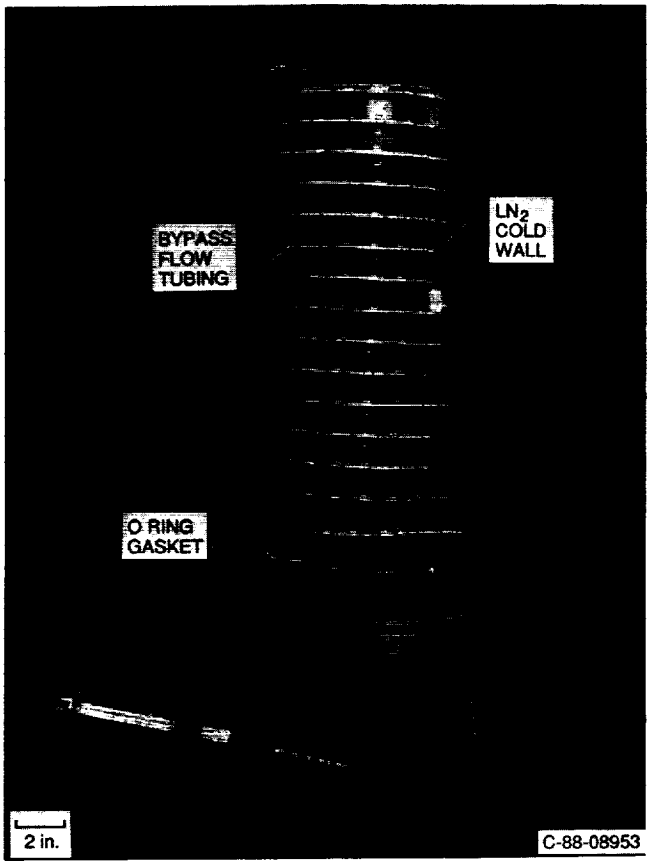

Figure 2. - LN_2 Joule-Thomson device test rig.

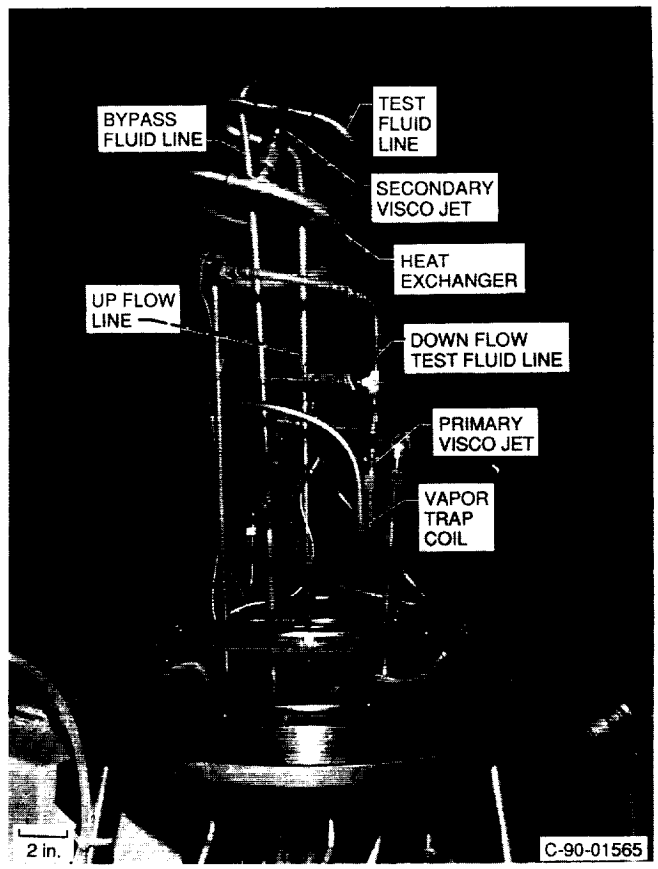

Figure 3. - Apparatus surrounded by the LN_2 cold wall.

VISCO JET DETAILS

(Taken from the Lee Technical Hydraulic Handbook)

An independent Visco "stage" consists of three different patterns which are combined to form a complex fluid passageway.

FLUID FLOW

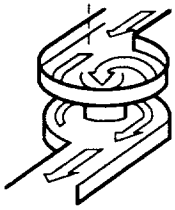

While passing through the tortuous path within each "stage" the fluid encounters various orifices and spin chambers, and changes direction of rotation many times.

The Lee Visco Jets contain a large number of spin chambers and tangential slots arranged in a series to provide a uniquely restrictive, tortuous path for the fluid medium. Flow enter each "stage" at the center of the pattern. From that point, it passes into a spin chamber via a rectangular slot. Within the chamber, the spinning liquid creates a back pressure which varies with the viscosity of the liquid. The liquid then passes through a restriction with a circular cross-section to the center of another spin chamber on the opposite face of the "stage". This spin chamber has an exiting tangential slot which is in the opposite direction from the previous entrance slot. The changing of direction forces the liquid to come to rest before it makes its exit from the deceleration chamber. This process is repeated within all the series of cavities of one "stage" until the liquid leaves through the final circular cross-section hole at the center of the pattern. Within practical limits, additional stages can be assembled to provide increased Lohm rating, or higher resistance to flow.

Some Lee Visco Jets are made from solid stainless steel discs, while others are fabricated from photo-etched stainless steel plates which are bonded together to produce a homogenous leak-proof product. All Visco elements are rigidly and permanently retained in their respective inserts, cartridges, or linemounts. Standard Lee Visco Jets are calibrated to the noted Lohm ratings in both directions. Lee Visco Jets with minimum passages of 0.032" or less are protected at each end by an appropriately sized filter screen.

Permission is hereby granted to use, copy and reproduce the general engineering material, including nomograms, tables and formulae, with the only restriction being to give credit to The Lee Company if the material is published or republished.

Figure 4.

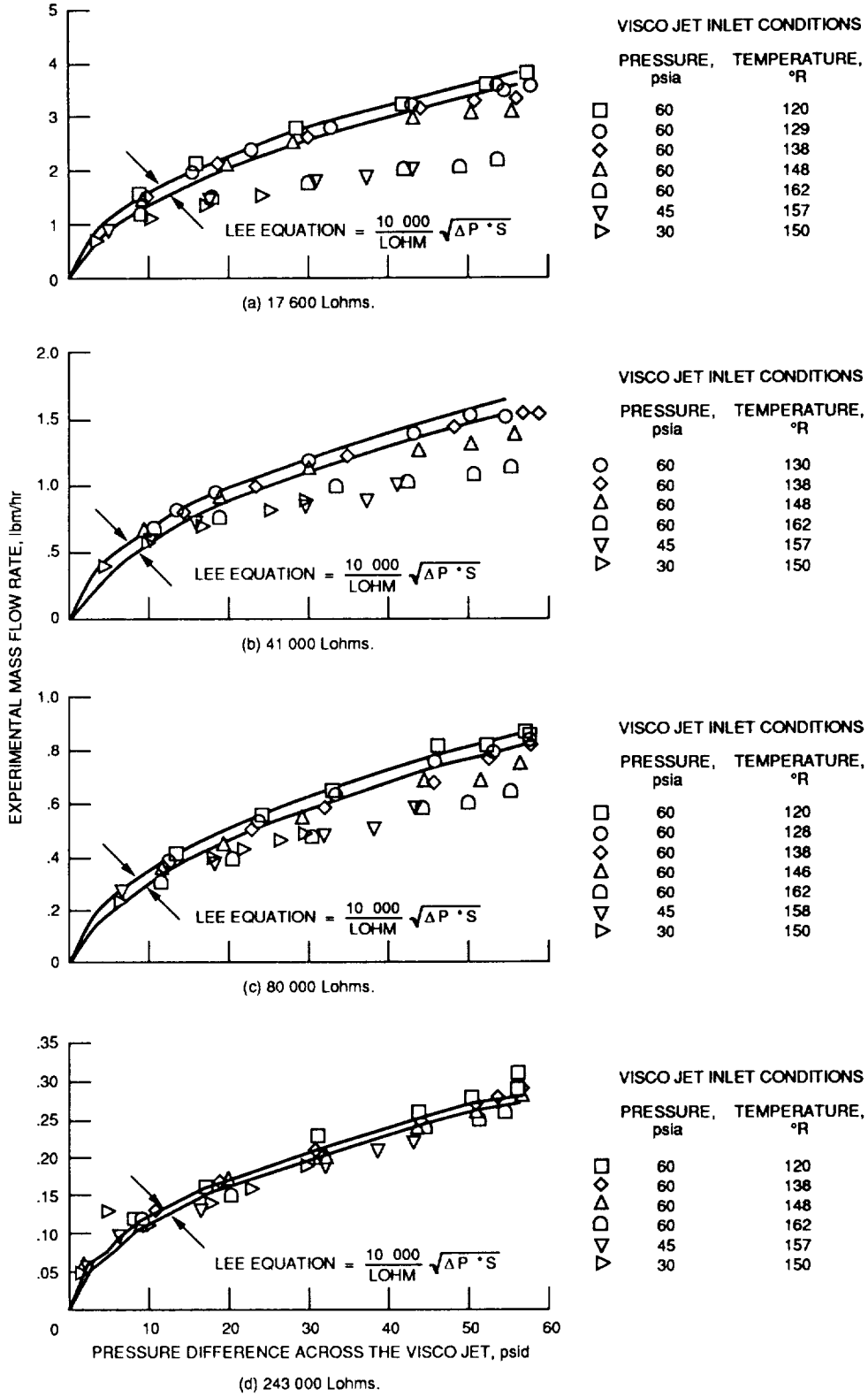

Figure 5. - Nitrogen flow through Visco Jet.

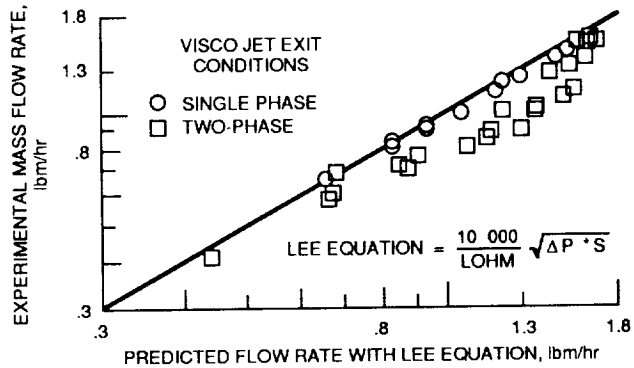

Figure 6. - Experimental and predicted values with Lee equation, 41 000 Lohm's.

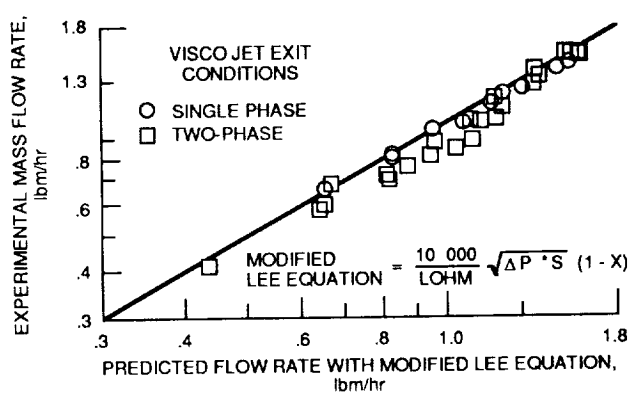

Figure 7. - Experimental and predicted values with modified Lee equation, 41 000 Lohm's.

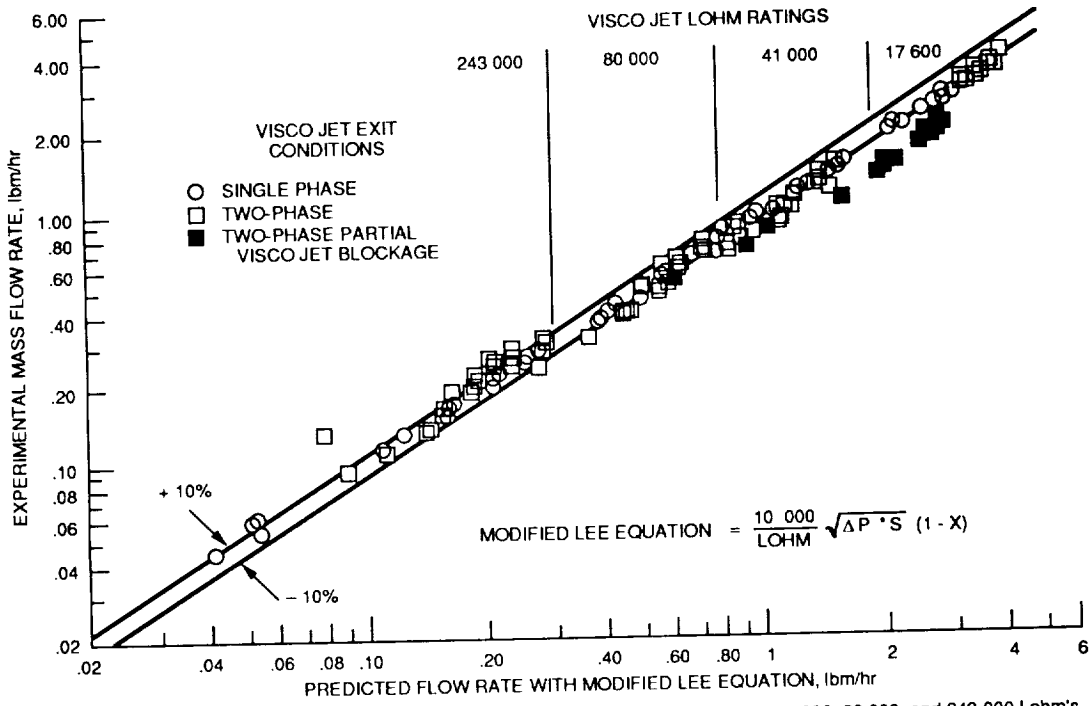

Figure 8. - Experimental and predicted values with modified Lee equation; 17 600, 41 000, 80 000, and 243 000 Lohm's.

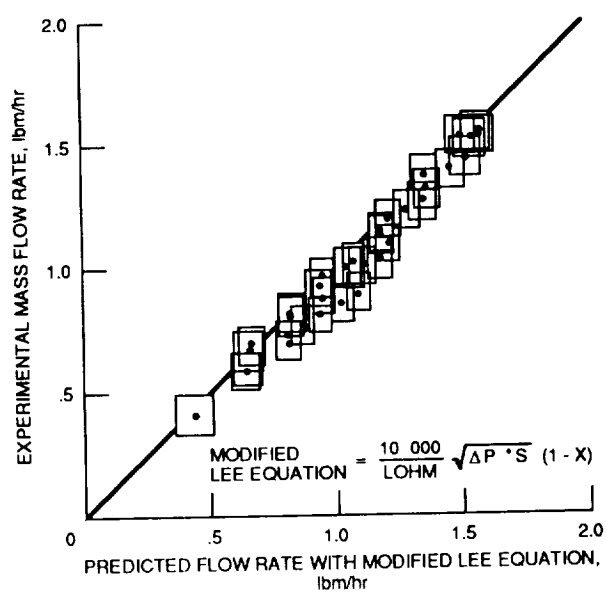

Figure 9. - Range of experimental and predicted values with modified Lee equation, 41 000 Lohm's.

NASA
National Aeronautics and Space Administration

Report Documentation Page

1. Report No. NASA TM-103121	2. Government Accession No.	3. Recipient's Catalog No.
4. Title and Subtitle: Acquisition and Correlation of Cryogenic Nitrogen Mass Flow Data Through a Multiple Orifice Joule-Thomson Device		5. Report Date: May 1990
		6. Performing Organization Code
7. Author(s): S. Stephen Papell, Naseem H. Saiyed, and Ted W. Nyland		8. Performing Organization Report No. E-5449
		10. Work Unit No. 591-21
9. Performing Organization Name and Address: National Aeronautics and Space Administration, Lewis Research Center, Cleveland, Ohio 44135-3191		11. Contract or Grant No.
		13. Type of Report and Period Covered: Technical Memorandum
12. Sponsoring Agency Name and Address: National Aeronautics and Space Administration, Washington, D.C. 20546-0001		14. Sponsoring Agency Code

15. Supplementary Notes

S. Stephen Papell, Analex Corporation, NASA Lewis Research Center, 21755 Brookpark Road, Fairview Park, Ohio 44126. Naseem H. Saiyed and Ted W. Nyland, NASA Lewis Research Center.

16. Abstract

Liquid nitrogen mass flow rate, pressure drop, and temperature drop data ~~have been~~ obtained for a series of multiple orifice Joule-Thomson devices, known as Visco Jets, over a wide range of flow resistance. The test rig used to acquire the data was designed to minimize heat transfer so that fluid expansion through the Visco Jets would be isenthalpic. The data include a range of fluid inlet pressures from 30 to 60 psia, fluid inlet temperatures from 118 to 164 °R, outlet pressures from 2.8 to 55.8 psia, outlet temperatures from 117 to 162 °R and flow rate from 0.04 to 4.0 lbm/hr of nitrogen. A flow rate equation supplied by the manufacturer was found to accurately predict single-phase (noncavitating) liquid nitrogen flow through the Visco Jets. For cavitating flow, the manufacturer's equation was found to be inaccurate. Greatly improved results were achieved with a modified version of the single-phase equation. The modification consists of a multiplication factor to the manufacturer's equation equal to one minus the downstream quality based on an isenthalpic expansion of the fluid across the Visco Jet. For a range of flow resistances represented by Visco Jet Lohm ratings between 17 600 and 80 000, 100 percent of the single-phase data and 85 percent of the two-phase data fall within ±10 percent of predicted values.

17. Key Words (Suggested by Author(s)): Cryogenic liquid; Isenthalpic expansion; Joule-Thomson device; Multiple orifices		18. Distribution Statement: Unclassified – Unlimited; Subject Category 34	
19. Security Classif. (of this report): Unclassified	20. Security Classif. (of this page): Unclassified	21. No. of pages: 22	22. Price*: A03

NASA FORM 1626 OCT 86

*For sale by the National Technical Information Service, Springfield, Virginia 22161